

This material is posted here with permission of the IEEE. Such permission of the IEEE does not in any way imply IEEE endorsement of any of the Alliance for Wireless Power's products or services. Internal or personal use of this material is permitted. However, permission to reprint/republish this material for advertising or promotional purposes or for creating new collective works for resale or redistribution must be obtained from the IEEE by writing to pubs-permissions@ieee.org<<mailto:pubs-permissions@ieee.org>>. By choosing to view this document, you agree to all provisions of the copyright laws protecting it.

Loosely-Coupled Wireless Power Transfer: Physics, Circuits, Standards

Kamil A. Grajski, Ryan Tseng and Chuck Wheatley

Qualcomm Incorporated

San Diego, CA, USA

Abstract — Loosely-coupled (LC) wireless power transfer (WPT) offers unique, next-generation improvements in user experience, and product design and innovation towards the vision of ubiquitous power, and infinite stand-by time for a wide range of consumer electronic devices. We outline the vision as it relates to today's mobile, battery-powered, hand-held, consumer electronics devices, and consider the unique capabilities of loosely-coupled (LC) WPT. We then describe the physics of the magnetically coupled resonant coil subsystem, which lies at the heart of LC WPT, discuss approaches and challenges in implementing WPT electronic circuits, and review industry progress towards timely, high-quality WPT technical standards.

Index Terms — wireless power transfer, loosely-coupled, electromagnetic coupling, magnetic resonance.

I. UBIQUITOUS POWER AND LC WPT

A multiplicity of factors contributes to the economic *utility* of mobile, battery-powered, hand-held consumer electronics devices. Onboard energy storage and power delivery are critical factors in hand-held form factor utility. Hardware advances, new radio technologies and next-generation operating systems enable new applications and services that mutually reinforce to drive up power demand. Increased power demand, in turn, drives up device real estate demand for a battery and related circuitry, and peripheral interfaces for DC power and charging. However, form factor (e.g., volume, weight, safety, aesthetics) ultimately limits availability of onboard energy storage for on-demand power.

The vision of ubiquitous power is to meet device energy demands for typical usage in a manner that is natural and transparent to the typical consumer, through interactions in a wireless power transfer (WPT) source-rich physical environment [1-3]. WPT source availability (WPT density) in the environment must be such that user-mediated average time between WPT sessions and user-mediated average WPT session duration are sufficient to meet energy demands.

Practically, ubiquitous power injects new flexibility into the design trade-off between onboard energy storage, form factor and utility. Suppose that for a fixed onboard energy storage requirement, a new battery technology reduces energy storage real estate required to $A \text{ mm}^2$. In the context of ubiquitous power, that reduction might be driven to $B \text{ mm}^2$, $B \ll A$. In the limit, $B \rightarrow 0$ for minimal onboard energy storage.

The vision of ubiquitous power encompasses a range of use cases and device types broad enough to admit multiple WPT approaches [3-6]. In this paper we focus on loosely-coupled WPT (LC WPT) defined as "... resonant wireless transfer of power... through magnetic induction between... coil(s) where the coupling factor (k) can be less than 0.1, though values up to 1 may also be supported, and where the system requires [coupled] magnetic resonance," [7]. LC WPT offers unique advantages, principally, freedom of device placement on the x-y plane of the charging source, and the ability to charge multiple devices simultaneously, among many other features [3, 8-11]. LC WPT additionally offers positioning flexibility in the z-direction. This enables embedded LC WPT in surfaces (e.g., work surfaces, home furnishings, public areas) or other complex form factors (e.g., automotive). Such flexibility is of critical importance to establishing an LC WPT source-rich environment.

II. PHYSICS OF LC WPT

A salient feature of LC WPT systems is a series resonance-tuned pair of magnetically-coupled coils. The magnetic coupling – electromagnetic induction – is determined by the mutual inductance between the coils.

While others have analyzed a variety of LC WPT configurations [10-17], we consider a simple case of a concentric pair of single-turn loops with radius r_i and r_o , resp., with $r_o \gg r_i$ and vertical displacement in air z . Faraday's Law

and Lenz's Law describe that a time-varying current in the outer loop (I_o) results in a time variation of the magnetic flux through the inner loop ($\Phi_{i,o}$) with the consequence that an e.m.f. ($\mathcal{E}_{i,o}$) is induced in the inner loop. In the case of finite load, $\mathcal{E}_{i,o}$ drives an inner loop current whose direction is such to induce an opposing e.m.f. in the outer loop; and thus, to oppose the time variation in magnetic flux $\Phi_{i,o}$.

Mathematically,

$$\mathcal{E}_{i,o} = -\frac{d\Phi_{i,o}}{dt} = -\frac{d}{dt} \int_S \mathbf{B}_o \cdot d\mathbf{A}_i \quad (1)$$

$$= -M \frac{dI_o}{dt} \quad (2)$$

where \mathbf{B}_o is the magnetic flux density produced by the current flow in the outer loop, $d\mathbf{A}_i$ is an area element on an open surface (S) defined by the inner loop, and M is the mutual induction between coils. The Biot-Savart law leads to an expression for the magnetic flux density \mathbf{B}_o at a field point \vec{r}_p (at height z above center on the loop axis):

$$\mathbf{B}_o = \oint_o d\mathbf{B}_o = \frac{\mu_o}{4\pi} I_o \oint_o \frac{d\vec{s} \times \hat{r}}{|\vec{r}|^3} = \frac{\mu_o I_o r_o^2}{2(r_o^2 + z^2)^{3/2}} \quad (3)$$

where $I_o d\vec{s}$ is the infinitesimal current source point on the outer loop, $|\vec{r}|$ is the magnitude of the displacement vector \vec{r} from current source point to the field point, \hat{r} is the unit vector in the direction of \vec{r} , μ_o is the permeability of free space, and the closed integral is around the outer loop. Combining (1), (2) and (3), and recalling the assumption $r_o \gg r_i$, we obtain an expression in purely geometric terms for mutual inductance:

$$M_{i,o} = \frac{\mu_o \pi r_o^2 r_i^2}{2(r_o^2 + z^2)^{3/2}} \quad (4)$$

Here, the coupling coefficient, $k_{i,o}$, as given by (5), is a derived rather than fundamental system property:

$$M_{i,o} = k_{i,o} \sqrt{L_i L_o} \quad (5)$$

In LC WPT the operating region $k \ll 1$ is made practical and efficient through resonance-tuning of the coils.

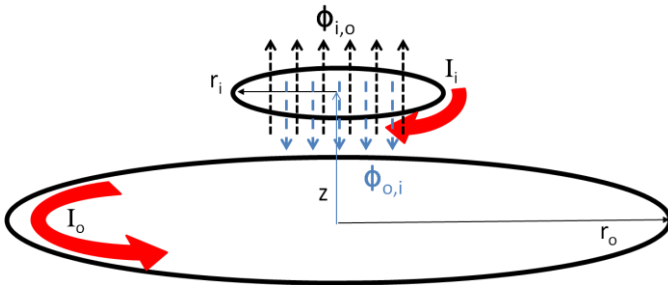


Fig. 1. Mutual inductance, a purely geometric factor, is fundamental to LC WPT. (Source drivers not shown.)

An idealized equivalent circuit model is used to analyze the power transfer efficiency of a resonance-tuned magnetically-coupled coil pair. In such a configuration, each coil is matched with a capacitance so as to share a common, high-Q oscillatory, resonant frequency, ω_o . Figure 2 illustrates such a circuit model, where V_{in} is the input voltage, R_1 , R_2 are the ohmic loss resistances in the inductors, C_1 , C_2 are the tuning capacitors, L_1 , L_2 are the inductance values at resonance (although as will be shown these self-inductances do not explicitly enter the power efficiency calculation), M is the mutual inductance, and R_L is the load resistance. Solving the pair of equations for loop currents leads to an expression for power transfer efficiency at perfect resonance $\omega = \omega_o$:

$$\eta = \frac{\omega_o^2 M^2 R_L}{(R_2 + R_L)(R_1(R_2 + R_L) + \omega_o^2 M^2)} \quad (6)$$

where power efficiency (η) is defined as the ratio of power delivered to R_L to the power delivered to the coil 1 whose resistive loss is R_1 .

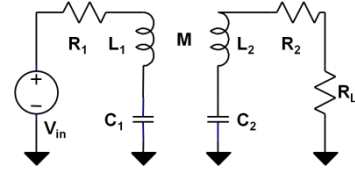


Fig. 2. Circuit model for analysis of power transfer efficiency at resonance for a pair of resonance-tuned magnetically coupled coils.

Power transfer efficiency at resonance through the circuit shown depends only on resonant frequency (ω_o), mutual inductance (M), coil loss resistances (R_1 , R_2), and load resistance (R_L). Figure 3 plots efficiency as a function of R_L for several values of mutual inductance from a representative early laboratory setup: $R_1=1.5\Omega$, $R_2=1.2\Omega$, $\omega_o=(2\pi*6.78 \times 10^6)$, $M=225-275\text{nH}$. As M varies, maximum efficiency occurs at different values of R_L . Setting the partial derivative of (6) with respect to R_L to zero, solving for R_L and confirming with the "second derivative test", gives an expression for the maximum efficiency as a function of load (optimal) R_L^* :

$$R_L^* = R_2 \sqrt{1 + \frac{\omega_o^2 M^2}{R_1 R_2}} \quad (7)$$

In this laboratory example, $R_L^* = 9.6$ and $M=250\text{nH}$, for a maximum efficiency for the circuit shown as 78%.

Substituting (7) into (6) gives a general expression for maximum power transfer efficiency between coils at resonance which, with further manipulation, is written as (8):

$$\eta^* = \left(\sqrt{1 + \frac{\omega_0^2 M^2}{R_1 R_2}} - 1 \right) / \left(\sqrt{1 + \frac{\omega_0^2 M^2}{R_1 R_2}} + 1 \right) \quad (8)$$

Define mutual quality factor, or coupling efficiency parameter,

$$Q_M = \omega_0 M / \sqrt{R_1 R_2} \quad (9)$$

and rewrite (8) in a more intuitive, accessible form:

$$\eta^* = \left(\sqrt{1 + Q_M^2} - 1 \right) / \left(\sqrt{1 + Q_M^2} + 1 \right) \quad (10)$$

The expression above shows that maximum power transfer efficiency between the coils at resonance is a monotonically increasing function of mutual quality factor. We see again that mutual inductance, resonant frequency, and ohmic losses in the coils play a fundamental role. Last, combining (5) and (10) we relate these fundamental variables with commonly employed derived descriptors, such as coupling coefficient:

$$Q_M = \frac{\omega_0 M}{\sqrt{R_1 R_2}} = \frac{\omega_0 k \sqrt{L_1 L_2}}{\sqrt{R_1 R_2}} = \omega_0 k \sqrt{Q_1 Q_2} \quad (11)$$

where $Q_j = \omega_0 L_j / R_j$, is the individual coil quality factor. In the present example, we measure $L_1 = 7.5 \mu\text{H}$ and $L_2 = 2.8 \mu\text{H}$, which, for the given values of M yields values for the coupling coefficient in the range $k = 0.049 - 0.06$. Thus, we confirm efficient power transfer in a low coupling coefficient regime.

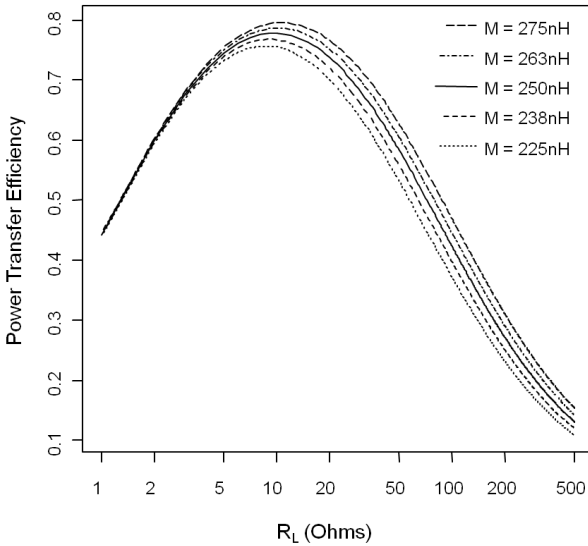


Fig. 3. Power transfer efficiency as a function of R_L and M (R_1 and R_2 fixed) for circuit in Figure 2 and power transfer efficiency by (6).

For maximum end-to-end efficiency of the circuit as a whole, the source (shown as V_{in} in Fig 2) must then be matched to coil 1, when R_L^* is at the value for maximum efficiency (as shown in Figure 3). The input impedance seen by the source is then a function of R_1 , R_2 and M :

$$Z_{in} = R_1 + \frac{\omega_0^2 M^2}{(R_2 + R_L^*)} \quad (12)$$

Figure 4 plots Z_{in} as a function of R_L for several values of M . In the present example, $R_L^* = 9.6$, $M = 250\text{nH}$, and $Z_{in} = 12\Omega$.

Not all aspects reviewed above generalize to LC WPT with simultaneous secondary (outer) loops. For example, the concept of mutual quality factor must take into account many more interactions, but to first order, such as when mutual inductance between secondary (outer) is low (due to physical separation), the mutual quality factor between source coil and secondary (outer) coil remains instructive.

In summary, physics of LC WPT consists of mutual inductance-maximizing geometric design in combination with tuned resonance to drive efficient power transfer between a source coil and load coil over separation distances comparable or in excess of the characteristic length of the source coil (in the present simple case, a vertical separation comparable to the radius of the outer loop) – even in a regime of low coupling coefficient (k).

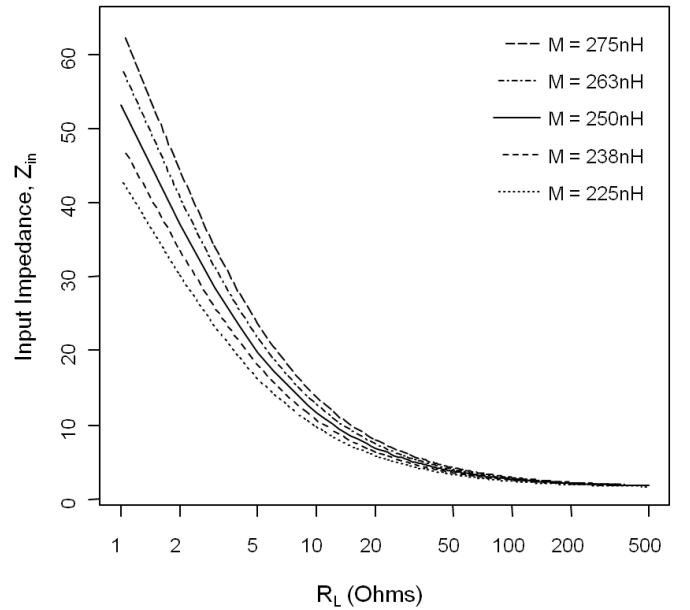


Fig. 4. Input impedance as a function of R_L and M , with R_1 , R_2 the same as used to generate Figure 3.

III. CIRCUITS FOR LC WPT SYSTEMS

LC WPT circuits are the bridge from magnetostatics to commercially viable products. As noted, an obvious feature of LC WPT systems is the coupled coils subsystem. But this subsystem operates within a larger end to end system whose primary purpose is the efficient transfer of power from a power source to load, such as a device-to-be-charged (DTBC)..

In the case of mobile, battery-powered consumer electronic devices, the design goal is made more complex owing to the fact that multiple DTBCs can charge at the same time, and each DTBC can see a different time-varying, charge state-dependent load. Figure 5 depicts the cascade of power transfer handling elements of a general LC WPT in an end to end functional model. Major system components include the source, the coupled coils, and the DTBC subsystems, together with the DTBC load. Each of these functional blocks contains subelements. Each subelement is analyzed in terms of its unique efficiency and impedance transformation and expressed as a function of the (charge state-dependent) load seen by that subelement.

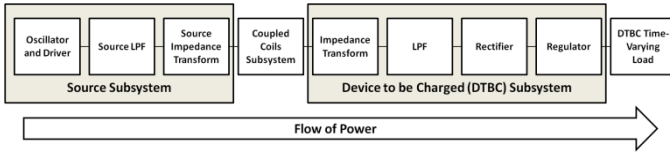


Fig. 5. LC WPT power handling end-to-end circuit functional block diagram. DTBC load is time-varying as a function of DTBC charging state. (Input voltage not shown.)

Figure 6 shows a model LC WPT application as a high-level circuit design. By inspection, one can appreciate the need to model, design and analyze LC WPT *as a system* as not all system (sub)elements operate at maximal efficiency at the same time throughout the typical DTBC charging cycle. Further, at the subelement level, power transfer efficiency is generally a nonlinear function of the (time varying) load.

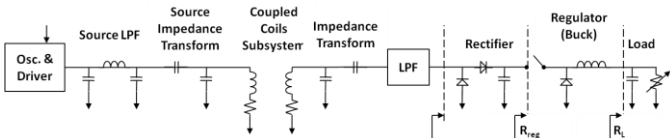


Fig. 6. Model LC WPT power handling high-level circuit model. The challenge for the LC WPT system designer is that load is not fixed. Load is a function of time varying charge state. Consequently, each element in the network must be described in terms of its own individual efficiency and impedance transformation as a function of the load that such element sees.

To illustrate but one such system-level dimension, consider power transfer through the LC WPT receiver subsystem at resonance as a function of the Buck regulator duty cycle. By adjusting the switching duty factor (δ), the regulator maintains load voltage at a designed-in value over the operating range.

We model an ideal switching regulator as $R_{\text{reg}} = R_L / \delta^2$. As the duty cycle increases, the value of R_{reg} tends towards that of R_L , such that in the limit of 100% duty cycle, the regulator is effectively shorted and $R_{\text{reg}} = R_L$. Referring to Figure 6, if all of the preceding elements in the receiver are ideal then, in particular, the source impedance of the rectifier (R_{rect}) is zero.

In such a case, power delivery to the load operates as expected. Namely, for a given load R_L , as duty cycle increases, R_{reg} drops, leading to greater power transfer. This is shown in Figure 7 top left.

Section II demonstrated that resistive losses in the coils comprising the coupled coils subsystem impact power transfer. In the present example, the effect of resistive losses in the receiver coil appears as a rectifier source impedance. To illustrate the interplay between rectifier source impedance, regulator operation and load, one can make a further abstraction of the receiver circuit shown in Figure 6, when at resonance, as a voltage source (V_s) connected to resistors (R_{rect}) and (R_{reg}) placed in series; a voltage divider circuit. In such a model, as duty cycle increases and R_{reg} tends towards R_L , then a condition may arise, depending upon the value of R_{rect} , where the power delivered *drops*. See Figure 7. The condition – power transfer collapse when R_{reg} reaches R_{rect} – occurs in the case of sufficiently high available (input) power.

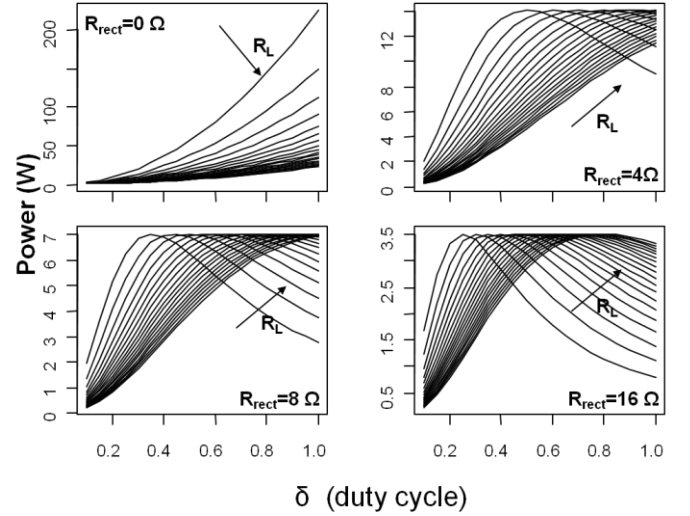


Fig. 7. Power transfer through the receiver subsystem, depends on load (R_L), rectifier source impedance (R_{rect}) and Buck regulator duty cycle (δ). Power collapse can occur when duty cycle saturates and effective load resistance falls below that of the rectifier source impedance. (Power collapse or failure to reach regulated voltage level can also occur in other circumstances (not discussed).) Arrows show direction of increasing R_L from 1Ω to 10Ω in steps of 0.5Ω ; $V_s=15V$. *Top-left*: Ideal case. *Top-right*: $R_{\text{rect}}=4\Omega$. *Bottom-left*: $R_{\text{rect}}=8\Omega$. *Bottom-right*: $R_{\text{rect}}=16\Omega$. As R_{rect} increases, maximum power drops (note y-axis scales).

The main condition that leads to saturation of the duty cycle is power demand by DTBC(s) that is in excess of system capability. System design must safeguard for these conditions.

In this section, we've provided a high level view of the challenges facing the LC WPT system circuit designer. While

there is a growing body of recent academic LC WPT research for low-power consumer applications [8-17], it should be noted that not dissimilar systems have been investigated, but typically for proprietary industrial and commercial applications [18-21]. In the consumer electronics segment, widespread adoption by manufacturers, and ultimately by consumers, often depends upon the availability of high-quality technical and interoperability standards, and stable and clear Regulatory policy and compliance frameworks.

IV. TECHNICAL STANDARDS FOR LC WPT

LC WPT technical standardization in a Standards Development Organization (SDO) typically considers LC WPT as a functional element within a larger WPT system. Figure 8 shows a functional block diagram of a WPT system that includes the LC WPT (power handling) system and its functional relationship to non-power handling elements.

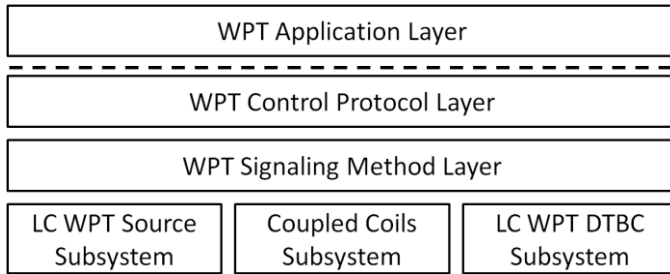


Fig. 8. WPT high-level system block diagram, including an LC WPT power handling subsystem. The scope of the typical SDO is confined to the layers below the WPT Application Layer.

The WPT Application Layer provides the interface point between the WPT System and its host (WPT Source or WPT DTBC), through hardware interfaces and a software applications programming interface (API).

The WPT Control Protocol Layer is responsible for managing the WPT system state machine including WPT “session management,” fault detection and safety, and processing input and output WPT signaling messages. Such messages can occur infrequently, such as WPT session initiation, or they may occur more frequently, such as intra-WPT session power-level reporting or adjustment messages. Proposed solutions take the form of a limited number of messages, with limited error detection and correction, and with the simplest addressing schemes.

The WPT Signaling Method Layer encompasses the physical layer aspects of delivering and receiving WPT Control Protocol messages. A key consideration is whether that physical layer is modulated onto the power carrier (in-band signaling, e.g., load modulation) or utilizes a separate

operating frequency (out-of-band signaling, e.g., BlueTooth, NFC, among many other options).

Table I lists SDOs and several SDO-level coordination groups whose activities in WPT also include LC WPT. SDOs are by no means focused exclusively on LC WPT. The CEA and TTA efforts, for example, are organized in parallel working group (WG) each with a specialized focus on a particular underlying WPT technology. Some SDOs are responding primarily to regulatory-driven questions, such as operating frequency considerations, EMC, RF emissions and safety (e.g., ETSI, CCSA). Other SDOs are focused directly on the development of LC WPT technical standards (CEA, BWF/ARIB, TTA). Still others are in the early stages, including processing New Work Item Requests (IEC, ISO/IEC JTC1) or developing initial Technical Reports (IEC). What is immediately obvious is the widespread international interest in WPT technical standardization. SDO-level coordination activities (GSC; CJK) should help promote the development of harmonized standards to the benefit of widespread adoption.

Table I. Global survey of LC WPT technical standards development.

Standards Development Organizations LC WPT Activities			
Name	Geography	Area of Interest	Status
GSC	Global	Technical Standards	GSC-16 Resolution on WPT
IEC TC 100	Global	Technical Standards	Stage 0 Project
ISO/IEC JTC1	Global	Technical Standards	SC6 NWI + IEC TC 100 Liaison
CJK	Asia	Regulatory + Technical Stds	CCSA, ARIB, TTA coordination
CEA	USA	Technical Standards	CEA R6.3 WG1-WG5
ETSI	Europe	Regulatory	ETSI TC ERM
CCSA	China	Regulatory	TC9 WG1 (EMC), WG3 (RF)
BWF/ARIB	Japan	Regulatory + Technical Stds	Framework Agreed
TTA	Korea	Regulatory + Technical Stds	PG709

Development of wireless power transfer technical standards takes place subject to applicable Regulations [22]. Regulations serve the purpose of protecting people and services in the areas of safety, efficient use of spectrum, harmful interference, and EMC (immunity). Compliance is established through standardized testing protocols, including direct measurement and simulation. Table II indicates the complexity of the Regulatory environment around WPT.

Table II. Global survey of LC WPT Regulatory environment.

Requirements	US	EU	International
Intentional Emission	FCC Part 18	EN 55011	CISRP 11
RF safety	CFR 47 Part 1, 2	EN 62311	ICNIRP 1998 & 2010
Conducted spurious emissions	FCC Part 18	EN 55011	CISRP 11
Radiated spurious emissions	FCC Part 18	EN 55011	CISRP 11
EMC Immunity	N/A	EN 61000-6-1	IEC 61000-6-1
Electrical safety	UL/CAN 60950	EN 60950	IEC 60950
WEEE/ROHS	CA ROHS	WEEE DIR/ROHS DIR	TBD
Labeling	FCC Part 2, 18	CE Mark	TBD

WPT Regulatory categorization is critical. Designs are subject to different Regulations depending on WPT operating frequency and signaling method (in-band or out-of-band; uni- or bi-directional). Industrial, Scientific and Medical (ISM) bands, e.g., 6.78MHz, defined by the ITU-R, are attractive for the WPT handling subsystem, because of global availability and unrestricted emissions, e.g., FCC Part 18.

Regulatory categorization drives RF exposure limits. WPT involves people in close proximity with the device near-field. Devices should be tested for Regulatory compliance in accordance with *basic restrictions* (i.e., based directly on established health effects) as in ICNIRP 1998 [23] and ICNIRP 2010 [24]. Restrictions are expressed as operating frequency-dependent limits on current density, specific energy absorption rate (SAR) and induced electric field.

Use case analysis is a critical navigational aid to WPT Regulations. It is straightforward to define “worst-case” scenarios whereby nearly any WPT approach exceeds limits. More challenging is to quantitatively define realistic use cases, including coil geometries, user position and orientation, power levels and product form factors, among many others. A clear set of use cases guides assessment early during the product R&D cycle, fosters development of form-factor accurate (FFA) prototypes that, in turn, enable direct measurement of radiated emissions and RF exposure levels, and establishes the basis for a simulation-based compliance testing methodology.

VI. CONCLUSION

The driving vision for LC WPT is ubiquitous power. Ubiquitous power holds the promise of new levels of device utility. Such increased functionality must not arrive at the cost of increased consumer anxiety and inconvenience over the basic requirement of power. To achieve the vision of ubiquitous power, the physics and circuits of LC WPT must be integrated in such a way as to support interoperable systems with demonstrated compliance with applicable Regulations. An available path is through industry participation in the development of globally harmonized,

timely, high quality Regulations, technical standards, interoperability specifications, minimum performance testing and certification, and regulatory compliance methodologies.

REFERENCES

- [1] A. Rahmati, A. Qian, and L. Zhong, “Understanding Human-Battery Interaction on Mobile Phones,” Human computer interaction with mobile devices and services, (MobileHCI '07), 2007 © ACM. doi: 10.1145/1377999.1378017.
- [2] D.Ferreira, A. K. Dey, and V. Kostakos, “Understanding Human-Smartphone Concerns: A Study of Battery Life,” Pervasive computing (Pervasive'11), Kent Lyons, Jeffrey Hightower, and Elaine M. Huang (Eds.). Springer-Verlag, Berlin, Heidelberg, 19-33.
- [3] M. Hunsicker, “The Future of Wireless Charging: Ubiquitous technology will enable anytime, anywhere recharging,” presented at the Image Sensors 2009 Wireless Power Summit, San Diego, CA, 2009.
- [4] A. Kurs, A. Karalis, R. Moffatt, J. D. Joannopoulos, P. Fisher, and M. Soljagic, “Wireless power transfer via strongly coupled magnetic resonances,” *Science*, vol. 317, no. 5834, pp. 83-86, Jun 7, 2007.
- [5] A. Karalis, J. D. Joannopoulos, and M. Soljagic, “Efficient wireless non-radiative mid-range energy transfer”, *Ann. of Phys.*, vol. 232, pp. 34-48, 2008.
- [6] *System Description Wireless Power Transfer, Volume I: Low Power, Part 1: Interface Definition, Version 1.0*, Wireless Power Consortium, July 2010.
- [7] *Wireless Power Glossary of Terms*, Consumer Electronics Association, CEA-2042.1, September 2011.
- [8] Z. N. Low, R. A. Chinga, R. Tseng and J. Lin, “Design and Test of a High-Power High-Efficiency Loosely Coupled Planar Wireless Power Transfer System,” *IEEE Trans. Ind. Electron.*, vol. 56, no. 5, pp. 1801-1812, May, 2009.
- [9] B. L. Cannon, J. F. Hoburg, D. D. Stancil, and S. C. Goldstein, “Magnetic Resonant Coupling As a Potential Means for Wireless Power Transfer to Multiple Small Receivers,” *IEEE Trans. Power Electron.*, vol. 24, no. 7, pp. 1819-1825, July, 2009.
- [10] D. Schatz, “Wireless Electricity Over Distance: Highly Resonant Magnetic Coupling,” presented at the Image Sensors 2009 Wireless Power Summit, San Diego, CA, 2009.
- [11] T. Imura and Y. Hori, “Maximizing Air Gap and Efficiency of Magnetic Resonant Coupling for Wireless Power Transfer Using Equivalent Circuit and Neumann Formula,” *IEEE Trans. Ind. Electron.*, vol. 58, no. 10, pp. 4746-4752, October, 2011.
- [12] Y. P. Su, X. Liu and S. Y. Ron Hui, “Mutual Inductance Calculation of Moveable Planar Coils on Parallel Surfaces,” *IEEE Trans. Power Electron.*, vol. 24, no. 4, April, 2009. doi: 10.1109/TPEL.2008.2009757.
- [13] K. Fotopoulou and B. W. Flynn, “Wireless Power Transfer in Loosely Coupled Links: Coil Misalignment Model,” *IEEE Trans. Magnetics*, vol. 47, no. 2, pp. 416-430, February, 2011.
- [14] H. Kim, D. Won and B. Jang, “Simple design method of wireless power transfer system using 13.56MHz loop antennas,” in *IEEE International Symposium on Industrial Electronics (ISIE)*, 2010 © IEEE. doi: 10.1109/ISIE.2010.5636910.
- [15] Shimokawa, S., et al., “A Numerical Study of Power Loss Factors in Resonant Magnetic Coupling,” in *IEEE MTT-S International Microwave Workshop Series on Innovative Wireless Power Transmission: Technologies, Systems, and Applications (IMWS)*, 2011 © IEEE. doi: 10.1109/IMWS.2011.5877134.
- [16] Y. Moriwaki, T. Imura, and Y. Hori, “Basic Study on Reduction of Reflected Power Using DC/DC Converters in Wireless Power Transfer

- System via Magnetic Resonant Coupling,” in IEEE 33rd International Telecommunications Energy Conference (INTELEC), 2011 © IEEE. doi: 10.1109/INTLEC.2011.6099737.
- [17] S. Kong, et al., “Analytical expressions for maximum transferred power in wireless power transfer systems,” in International Symposium on Electromagnetic Compatibility (EMC), 2011 © IEEE. doi: 10.1109/IEMC.2011.6038340.
- [18] Laouamer, R., et al, “A multi-resonant converter for non-contact charging with electromagnetic coupling,” in 23rd Intl Conf on Indust. Electron., Control and Instr. (IECON97), Nov. 1997, vol. 2, pp. 792-797. doi: 10.1109/IECON.1997.671998.
- [19] J. T. Boys, G. A. Covic and A. W. Green, “Stability and control of inductively coupled power transfer systems,” Proc. IEE – Elect. Power Applicat., vol. 147, no. 1, pp. 37-43, Jan. 2000. doi: 10.1049/ip-epa:20000017.
- [20] O. H. Stielau and G. A. Covic, “Design of loosely coupled inductive power transfer systems,” in Proc. 2000 Int. Conf. Power System Tech., vol. 1, pp. 85-90, Dec. 2000. doi: 10.1109/ICPST.2000.900036.
- [21] C. Wang, G. A. Covic and O. H. Stielau, “Design and test of a high-power high-efficiency loosely coupled planar wireless power transfer system,” IEEE Trans. Industr. Electronics, vol. 56, no. 5, May 2009. doi: 10.1109/TIE.2008.2010110.
- [22] P. Guckian, “Understanding wireless power regulation,” presented at the Wireless Power Summit, San Jose, CA, 2011.
- [23] International Commission on Non-Ionizing Radiation Protection. Guidelines for limiting exposure to time-varying electric, magnetic, and electromagnetic fields (up to 300 GHz). Health Phys, 74:494 –522, 1998.
- [24] International Commission on Non-Ionizing Radiation Protection. Guidelines for limiting exposure to time-varying electric, magnetic, and electromagnetic fields (1Hz-100kHz). Health Phys, 99:818 - 836, 2010